Am J Physiol Cell Physiol 288: C185–C194, 2005.
First published September 15, 2004; doi:10.1152/ajpcell.00207.2004.

Intracellular signaling specificity in response to uniaxial vs. multiaxial stretch: implications for mechanotransduction

Troy A. Hornberger,[1] Dustin D. Armstrong,[1] Timothy J. Koh,[1] Thomas J. Burkholder,[2] and Karyn A. Esser[1]

[1]*University of Illinois at Chicago, School of Kinesiology, Chicago, Illinois; and*
[2]*Georgia Institute of Technology, School of Applied Physiology, Atlanta, Georgia*

Submitted 27 April 2004; accepted in final form 9 September 2004

Hornberger, Troy A., Dustin D. Armstrong, Timothy J. Koh, Thomas J. Burkholder, and Karyn A. Esser. Intracellular signaling specificity in response to uniaxial vs. multiaxial stretch: implications for mechanotransduction. *Am J Physiol Cell Physiol* 288: C185–C194, 2005. First published September 15, 2004; doi:10.1152/ajpcell.00207.2004.—Several lines of evidence suggest that muscle cells can distinguish between specific mechanical stimuli. To test this concept, we subjected C_2C_{12} myotubes to cyclic uniaxial or multiaxial stretch. Both types of stretch induced an increase in extracellular signal-regulated kinase (ERK) and protein kinase B (PKB/Akt) phosphorylation, but only multiaxial stretch induced ribosomal S6 kinase ($p70^{S6k}$) phosphorylation. Further results demonstrated that the signaling events specific to multiaxial stretch ($p70^{S6k}$ phosphorylation) were elicited by forces delivered through the elastic culture membrane and were not due to greater surface area deformations or localized regions of large tensile strain. Experiments performed using medium that was conditioned by multiaxial stretched myotubes indicated that a release of paracrine factors was not sufficient for the induction of signaling to $p70^{S6k}$. Furthermore, incubation with gadolinium(III) chloride (500 μM), genistein (250 μM), PD-98059 (250 μM), bisindolylmaleimide I (20 μM), or LY-294002 (100 μM) did not block the multiaxial stretch-induced signaling to $p70^{S6k}$. However, disrupting the actin cytoskeleton with cytochalasin D did block the multiaxial signaling to $p70^{S6k}$, with no effect on signaling to PKB/Akt. These results demonstrate that specific types of mechanical stretch activate distinct signaling pathways, and we propose that this occurs through direct mechanosensory-mechanotransduction mechanisms and not through previously defined growth factor/receptor binding pathways.

growth; hypertrophy; muscle; strain; tension

THE INTRINSIC ABILITY of striated muscle cells to sense and respond to mechanical signals has been recognized for decades, and these responses have been implicated in a variety of biological processes ranging from organogenesis to regulation of tissue and cell size and, in cardiac tissue, the development of pathological disease (9, 15, 18, 22, 37). In addition to being able to sense mechanical signals, there is also evidence to suggest that muscle cells have the capacity to distinguish between different types of mechanical signals. For example, in skeletal muscle, chronic longitudinal stretch produces growth in length, defined by increased sarcomere number in series, whereas functional overload produces cross-sectional growth, as defined by increased sarcomere number in parallel (32). Growth in the heart also provides an example of different phenotypic responses to mechanical loading, with pressure overload resulting in increased ventricular wall thickness in contrast to volume overload resulting in increased ventricular volume (4). These examples highlight the evidence that in striated muscle tissue, different types of mechanical loading can produce distinct downstream adaptations. Furthermore, these examples suggest that specific cellular mechanisms may exist to sense and subsequently respond to the different mechanical forces delivered. However, because of the complexity of the mechanical environment within muscle tissue, the concept that different types of mechanical forces can elicit unique molecular events has not been well studied.

Defining the mechanical environment within a single muscle cell is technically very difficult, if not impossible, in vivo. This is because of numerous anatomical factors that include characteristics such as fiber orientation within the muscle (i.e., angle of pinnation), interactions between the muscle fiber and its own extracellular matrix/basal lamina, and the mechanical impact that results from the complex recruitment of motor units so that an activated muscle fiber from one motor unit will be contracting next to an inactive fiber from a different, nonrecruited motor unit. All of these factors contribute to both the magnitude and the type of forces experienced by a single muscle fiber within the tissue in vivo. Thus, to study mechanotransduction-mechanosensory capacities of muscle cells, it is necessary to apply clearly defined mechanical stimuli, and for this we rely on the use of in vitro mechanical stimulators (stretch devices). These devices can be used within the confines of a cell culture environment, and the mechanical stimuli that are delivered to the culture membrane are easily controlled and can be readily defined.

In vitro stretch devices can generally be grouped into one of two classes, uniaxial or multiaxial. The major difference between a uniaxial and multiaxial stretch device is the type of mechanical deformation delivered to the elastic culture membrane. In this study, we utilized these two types of devices in an attempt to identify whether muscle cells have the fundamental ability to differentiate between different types of mechanical forces. Alterations in well-known signaling molecules were evaluated as a means to discern whether differential mechanotransduction-mechanosensory information was being processed. The molecules evaluated included the extracellular signal-regulated kinase (ERK), protein kinase B (PKB/Akt), and the 70-kDa S6 kinase ($p70^{S6k}$). These signaling molecules were selected because previous reports have shown them to respond to mechanical stimuli and because they all have been

Address for reprint requests and other correspondence: K. Esser, Dept. of Physiology, Univ. of Kentucky, Albert B. Chandler Medical Center, 800 Rose St., Lexington, KY 40536-0298 (E-mail: karyn.esser@uky.edu).

The costs of publication of this article were defrayed in part by the payment of page charges. The article must therefore be hereby marked "*advertisement*" in accordance with 18 U.S.C. Section 1734 solely to indicate this fact.

implicated in the regulation of mechanical load-induced hypertrophy (1, 36).

The findings from these studies demonstrate that both uniaxial and multiaxial stretch induce an increase in PKB/Akt and ERK phosphorylation but that only multiaxial stretch induces an increase in $p70^{S6k}$ phosphorylation. Evidence is provided suggesting that the unique activation of $p70^{S6k}$ is a result of myotubes sensing multiaxial vs. uniaxial tensile strains and is not due to differences in surface area deformation or shear stress. In addition, our findings demonstrate that disrupting the actin cytoskeleton inhibits the multiaxial stretch-induced phosphorylation of $p70^{S6k}$, whereas pharmacological inhibitors that have been reported to block signaling to $p70^{S6k}$ after growth factor stimulation did not (6, 11, 12, 25). These findings suggest that a novel signaling pathway is used by multiaxial stretch to induce phosphorylation of $p70^{S6k}$. It is also important to note that although disruption of the actin cytoskeleton blocked the multiaxial stretch-induced phosphorylation of $p70^{S6k}$, it had no effect on the signaling to PKB/Akt, leading to the additional conclusion that mechanical stimuli can activate distinct mechanosensory-mechanotransduction pathways and that the activation of these pathways is specific to the types of mechanical forces applied.

MATERIAL AND METHODS

Materials. Peroxidase-conjugated anti-rabbit was purchased from Vector Laboratories (Burlingame, CA). FITC-conjugated anti-rabbit was purchased from Jackson Laboratories (Bar Harbor, ME). Phosphospecific (threonine-202/tyrosine-204) ERK1/2, (serine-473) PKB/Akt, and (threonine/serine-421/424) $p70^{S6k}$ were purchased from Cellular Signaling (Lake Placid, NY). Polyvinylidene difluoride (PVDF) membranes were purchased from Millipore (Bedford, MA). Enhanced chemiluminescence (ECL) detection reagent was purchased from Amersham Pharmacia Biotech (Amersham, UK). The DC protein assay kit was purchased from Bio-Rad (Hercules, CA). Dulbecco's modified Eagle's medium (DMEM), fetal bovine serum (FBS), and horse serum (HS) were purchased from Invitrogen (Carlsbad, CA). Cytochalasin D, gadolinium, genistein, and anti-α-actinin antibody were purchased from Sigma (St. Louis, MO). PD-098059, bisindolylmaleimide I (BIM), and LY-294002 were purchased from Calbiochem (San Diego, CA).

Cell culture. C_2C_{12} skeletal myotube cultures were grown by plating C_2C_{12} myoblasts on type I collagen-coated Bioflex membranes (Flexcell International, Hillsborough, NC) at a density of $\sim 1.5 \times 10^4$ cells/cm^2 as previously described (17). Myoblasts were maintained in low-glucose DMEM supplemented with antibiotics (100 μg/ml streptomycin and 100 U/ml penicillin; Sigma) and 10% FBS. Upon confluence (~48 h), cells were switched to DMEM supplemented with antibiotics and 10% HS to promote differentiation. Cells were maintained in this medium for 24 h and then switched back to the 10% FBS medium for an additional 5–6 days, after which distinct multinucleated myotubes were present. Media were changed every 48 h, and fresh medium was added 18 h before the initiation of mechanical stretch. Three hours before the initiation of stretch, culture plates were removed from the incubator, rapidly placed on the uniaxial or multiaxial stretch device, and returned to the incubator.

Mechanical stretch. Two separate devices were used to stretch the C_2C_{12} myotube cultures. The uniaxial stretch device consisted of a slight modification of the device described by Clark et al. (5). This is a motor-driven system that applies uniaxial stretch to a rectangle-shaped membrane. The sides of the membrane are unconstrained, so there is minor compression transverse to the direction of applied stretch. This is a feature of incompressibility and is very similar to what would happen if an isolated cell were stretched on a single axis. The multiaxial device (FX-3000; Flexcell International, Hillsborough NC) is a vacuum-operated system that produces nonuniform multiaxial (radial and circumferential) tensile strains with very little compression on a circle-shaped membrane (7). The airflow through the stretch plates is unrestricted, which diminishes the potential for internal pressure gradients in the cell culture plates. This is important because it allows the rate of deformation of the membrane to be a true reflection and a result of the rate of pressure change via the vacuum system.

The stretch programs employed in both devices were designed to produce cyclic 15% membrane stretch, cyclic 11% increases in membrane surface area (ΔSA) or cyclic 24% ΔSA. These changes were produced at a frequency of 1 Hz in a triangular wave form. Stretch cycles were sustained for 45 s followed by 15 s of rest. This pattern was repeated for a total of 10 min.

The ΔSA produced by the uniaxial stretch device was calculated from previously generated finite analysis (5). These data indicate that a 15% and 32% stretch along the major axis of the membrane produces an 11% and 24% ΔSA, respectively. The calculations for ΔSA produced by the multiaxial stretch device were based on spherical deflection geometry in which ΔSA is represented by a spherical cap (described below) (2). These calculations indicate that 7% and 15% membrane stretch produce an 11% and 24% ΔSA, respectively.

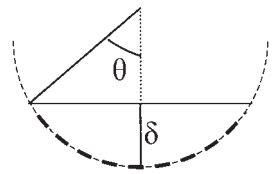

$$\Delta SA = [2\pi r^2(1 - \cos\theta) - (\pi r^2)] \times 100$$

$$r = (R^2 + \delta^2)/2\delta = \text{radius of curvature},\ \theta = \arcsin(R/r)$$

$$l_f = r\theta = \text{stretched membrane length}$$

$$l_o = R = 17.5\ \text{mm} = \text{resting membrane radius},\ \%\text{stretch} = [(l_f - l_o)/l_o] \times 100$$

$$\delta = \text{length of center point deflection extrapolated from applied vacuum pressure}$$

Application of fluid shear stress. Skeletal myotubes grown on type I collagen-coated Bioflex membranes were subjected to 10 min of fluid shear with the use of an orbital shaker in the incubator (Armalab, Bethesda, MD) as described by Kraiss et al. (23). This technique produces nonuniform laminar shear with the majority of cells being exposed to near-maximal (peak) shear stress (τ_{max}), which can be calculated as

$$\tau_{max} = a\sqrt{\rho\eta(2\pi f)^3}$$

where a is the radius of orbital rotation (1.27 cm), ρ is the density of the culture medium (1.0 g/cm^3), η is the viscosity of the medium (0.01 g·cm^{-1}·s^{-1}) (3), and f is the frequency of rotation (rotations/s) (23). At a frequency of 1 Hz (1 rotation/s), $\tau_{max} = 2.0$ dyn/cm^2.

Western blot analysis. Skeletal myotubes were collected in lysis buffer (20 mM Tris, pH 7.5, 150 mM NaCl, 1 mM EDTA, 1 mM EGTA, 1% Nonidet NP-40, 1 mM β-glycerol phosphate, 1 mM Na_3VO_4, 1 μg/ml leupeptin, and 1 mM PMSF) and measured for protein concentration with the DC protein assay kit. From the myotube homogenate, samples containing 10–60 μg of protein were dissolved in Laemmli buffer and subjected to electrophoretic separation by SDS-PAGE on 7.5% acrylamide gels as previously described (16). After electrophoretic separation, proteins were transferred to a PVDF membrane, blocked in 5% blotto [5% powdered milk in TBST (Tris-buffered saline, 1% Tween 20)] for 3 h followed by an overnight

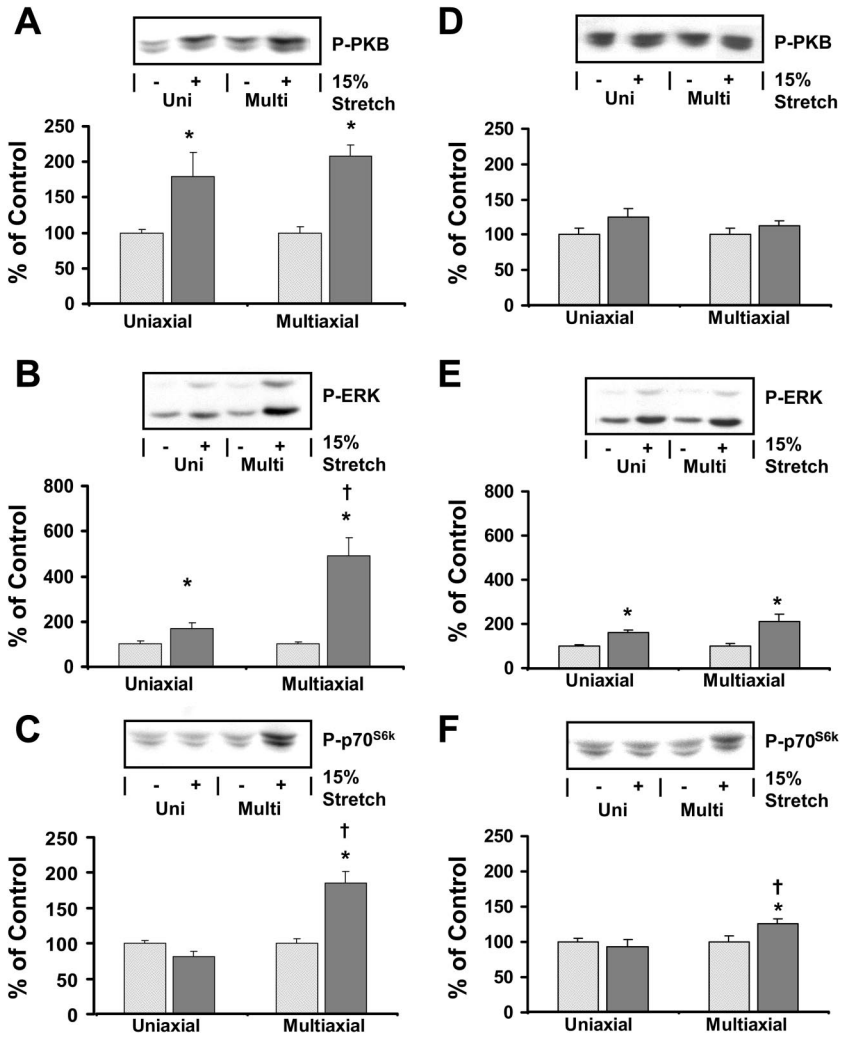

Fig. 1. Uniaxial and multiaxial stretch induces distinct signaling events. C_2C_{12} myotubes were subjected to 10 min (*A–C*) or 60 min (*D–F*) of 15% cyclic (1 Hz) uniaxial or multiaxial membrane stretch. Cell homogenates were separated by SDS-PAGE, and Western blotting was performed with phosphospecific antibodies to PKB/Akt (P-PKB; *A* and *D*), ERK1/2 (P-ERK; *B* and *E*), and $p70^{S6k}$ (P-$p70^{S6k}$; *C* and *F*). Values are presented as means ± SE and expressed as a percentage of control (n = 11–13/group) from 3–4 independent experiments. Control samples are represented as light shaded bars, and stretched samples are represented as dark shaded bars. Uni, uniaxial stretch; multi, multiaxial stretch. *Significantly different from control ($P \leq 0.05$). †Significantly different from uniaxial stretch ($P \leq 0.05$).

incubation at 4°C with primary antibody. After overnight incubation, membranes were washed for 30 min in TBST and then probed with anti-rabbit antibody for 45 min at room temperature. After another 30 min of washing in TBST, the blots were developed with ECL. Once the appropriate image was captured, membranes were stained with Coomassie blue to verify equal loading in all lanes. Densitometric measurements were carried out using the FluorSmax Imager with QuantityOne software (Bio-Rad). It should be noted that PKB/Akt and $p70^{S6k}$ contain multiple phosphorylation sites and that the phosphospecific antibodies against these proteins often reveal a doublet or triplet banding pattern (see Figs. 1–7). The doublet and triplet banding pattern likely reflects changes in mobility that result from different phosphorylation states of the protein; thus, when images were quantified, all of the doublet and triplet bands were counted as a single entity. The phosphospecific ERK antibody reveals two distinct bands that represent ERK1 (44 kDa) and ERK2 (42 kDa). For quantification, both ERK1 and ERK2 were each counted as a single entity.

Immunohistochemistry. C_2C_{12} myotubes were subjected to 10 min of cyclic 15% multiaxial stretch and immediately washed two times with ice-cold PBS, fixed in 4% paraformaldehyde for 10 min, and permeabilized with PBS containing 0.5% Triton X-100 for 10 min. Permeabilized cultures were blocked with PBS containing 1% bovine serum albumin (BSA) and 10% HS for 60 min, followed by an overnight incubation with primary antibody in 1% BSA at 4°C. The following dilutions of primary antibody were used: anti-α-actinin (1:2,000) and anti-$p70^{S6k}$ 421/424 (1:50). After incubation, the myotubes were washed four times with 1% BSA-PBS and then incubated with FITC-conjugated secondary antibody (1:100) for 1 h at room temperature. After another series of washes in 1% BSA-PBS, cultures were covered with Vectashield mounting medium (Vector Laboratories, Burlingame, CA), and a continuous series of images was constructed from individual images taken with identical exposure times. After an individual image was captured, the culture plate was moved with a micromanipulator, with care taken to keep a portion of the previous field in view. The overlapping fields from each exposure were used to reconstruct the continuous series of images. In other experiments, C_2C_{12} myotubes were grown on six-well plastic dishes (Corning, NY), fixed and permeabilized as described above, and incubated with fluorescein-conjugated phalloidin from Molecular Probes (Eugene, OR) in PBS (1:40). All immunofluorescent images were captured on a Kodak DC290 camera taken through a Nikon Diaphot 200 microscope and imported into Adobe Photoshop for analysis.

Pharmacological inhibitors. Before initiation of stretch, culture medium was replaced with DMEM containing 10% FBS and vehicle (DMSO) or 10 μM cytochalasin D, 500 μM gadolinium(III) chloride, 250 μM genistein, 50 μM PD-98059, 20 μM BIM, or 100 μM LY-294002. The concentration for each of the inhibitors employed was based on previously published work and testing that preceded the stretch experiments (8, 21, 24, 29). After a 45-min preincubation, myotubes were subjected to 10-min cyclic 15% multiaxial stretch as described above and then collected for Western blot analysis.

Conditioned media. C_2C_{12} myotubes grown on type I collagen-coated Bioflex membranes were placed in serum-free DMEM (serum starved) for 90 min, followed by the addition of fresh serum-free medium immediately before the 10 min of 15% cyclic (1 Hz) multiaxial stretch or static conditions were initiated. The conditioned medium from static or stretched myotubes was immediately removed and placed on a new set of serum-starved myotubes for 10 min. Myotubes were subjected to Western blot analysis as described above.

Statistical analysis. All values are expressed as means ± SE. Statistical significance was determined by ANOVA followed by Student-Newman-Keuls post hoc analysis. Differences between groups were considered significant if $P \leq 0.05$.

RESULTS

Uniaxial and multiaxial stretch induce distinct signaling events. Uniaxial and multiaxial stretch devices deliver different types of mechanical forces to the cell culture membrane. The uniaxial stretch device employed in this study produced a single axis of uniform tensile strain associated with a small magnitude of compression (5), whereas the multiaxial device produced nonuniform tensile strain through two axes (radial and circumferential) (7). In an effort to determine whether C_2C_{12} myotubes could distinguish between the different forces produced by the uniaxial and multiaxial stretch devices, alterations in the phosphorylation of signaling molecules PKB/Akt, ERK, and $p70^{S6k}$ were assessed after 10 min of 15% cyclic (1 Hz) stretch. At 10 min, both types of stretch induced a similar increase in PKB/Akt serine-473 (Fig. 1*A*) and threonine-308 phosphorylation (data not shown). Stretch on both devices also produced an increase in ERK phosphorylation, but the increase in ERK phosphorylation induced by multiaxial stretch was significantly greater in magnitude than the increase produced by uniaxial stretch (Fig. 1*B*) ($P \leq 0.05$). Only multiaxial stretch induced an increase in $p70^{S6k}$ phosphorylation (Fig. 1*C*). The multiaxial stretch-specific increase in $p70^{S6k}$ phosphorylation was evident with $p70^{S6k}$ threonine/serine-421/424 (Fig. 1*C*) and $p70^{S6k}$ threonine-389 phosphospecific antibodies, as well as with changes in gel mobility of total $p70^{S6k}$ (data not shown). It should be noted that multiaxial stretch-specific increase in glycogen synthase kinase-3β (GSK-3β) serine-9 phosphorylation was also observed (data not shown).

To determine whether the differences in signaling events between uniaxial and multiaxial stretch were the result of differences in the time course of activation, we assessed alterations in the phosphorylation of PKB/Akt, ERK, and $p70^{S6k}$ after 60 min of 15% cyclic (1 Hz) stretch. The results from these experiments indicated that PKB/Akt serine-473 phosphorylation was not elevated after 60 min or either uniaxial or multiaxial stretch (Fig. 1*D*). Furthermore, at 60 min, both uniaxial and multiaxial stretch produced a similar change in ERK phosphorylation (Fig. 1*E*), whereas only multiaxial stretch produced a significant increase in $p70^{S6k}$ threonine/serine-421/424 phosphorylation (Fig. 1*F*).

Stretch-sensitive signaling events are not responsive to fluid shear stress. The initial results of this study suggested that the multiaxial stretch-specific signaling events were the result of differences in the mechanical forces delivered through the elastic culture membrane. However, cyclic stretch produces motions in the overlying culture medium that, in turn, exert reactive forces (fluid shear stress) on the myotube culture. A variety of cell types are sensitive to fluid shear stress, and signaling events characteristic of this response include increases in ERK and $p70^{S6k}$ phosphorylation (19, 23). This effect is cell-type specific and dependent on the magnitude of fluid shear stress applied; for example, an increase in the magnitude of fluid shear stress produces an increase in the magnitude of phosphorylation (19, 23). In an effort to establish whether any of the signaling events induced by cyclic stretch were a result of fluid shear stress, myotube cultures were subjected to 10 min of 2 dyn/cm^2 peak fluid shear stress on an orbital rotary shaker at 1 Hz frequency. This magnitude of fluid shear stress is up to fourfold that produced during cyclic 1 Hz, 7% stretch (11% ΔSA) on the multiaxial device (3). Subjecting the myotubes to fluid shear stress did not alter PKB/Akt, ERK, or $p70^{S6k}$ phosphorylation (Fig. 2, *A–C*). These results suggest that the signaling events induced by cyclic stretch evolved independently of fluid shear stress and therefore were the result of the mechanical forces delivered through the elastic culture membrane. However, it should be noted that the cellular response to shear stress depends on both the magnitude of shear stress and the type of shear stress (static vs. pulsatile).

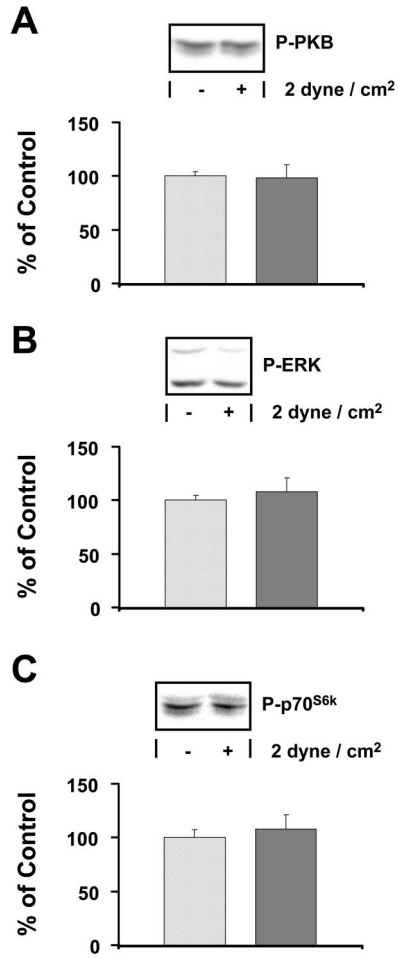

Fig. 2. Stretch-sensitive signaling events are not activated by fluid shear stress. C_2C_{12} myotubes were subjected to 10 min of 2.0 dyn/cm^2 peak fluid shear stress. Cell homogenates were separated by SDS-PAGE, and Western blotting was performed with phosphospecific antibodies P-PKB (*A*), P-ERK (*B*), and P-$p70^{S6k}$ (*C*). Values are presented as means ± SE and expressed as a percentage of control ($n = 6$/group) from 3 independent experiments. Controls samples are represented as light shaded bars, and sheared samples are represented as dark shaded bars.

The orbital rotary shaker used in this study produces static flow with a constant rate of fluid shear stress, whereas cyclic stretch produces pulsatile shear stress, and therefore we cannot fully rule out the possibility that shear stress may have contributed to the signaling events produced by cyclic stretch.

Different signaling events induced by uniaxial and multiaxial stretch are not due to differences in the magnitude of surface area deformation. One of the major differences in the mechanical forces produced by stretch on the uniaxial and multiaxial devices is the magnitude or dose of surface area deformation (ΔSA) produced by a given amount of stretch. As a result of transverse compression, uniaxial 15% stretch produces an 11% ΔSA, whereas 15% stretch on the multiaxial device produces a 24% ΔSA. To determine whether the differences in signaling events after 15% stretch on the uniaxial and multiaxial devices resulted from differences in the magnitude of ΔSA, the magnitude of uniaxial stretch was increased to 32%, which produced a 24% ΔSA, and the magnitude of multiaxial stretch was decreased to 7%, which produced an 11% ΔSA (see MATERIALS AND METHODS for calculations). These alterations allowed for the comparison of uniaxial and multiaxial stretch-induced signaling events at both 11% and 24% ΔSA.

The increase in PKB/Akt phosphorylation after both 11% and 24% cyclic ΔSA was similar on both devices (Fig. 3, *A* and *D*). Cyclic 11% ΔSA induced similar increases in ERK phosphorylation on the uniaxial and multiaxial devices (Fig. 3*B*). However, cyclic 24% ΔSA elicited a greater increase in ERK phosphorylation on the multiaxial compared with the uniaxial device (Fig. 3*E*; $P \leq 0.05$). Only stretch on the multiaxial device produced an increase in $p70^{S6k}$ phosphorylation, and this effect was observed after both 11% and 24% ΔSA (Fig. 3, *C* and *F*). Thus, despite normalizing for ΔSA, the differences in signaling events produced by the uniaxial and multiaxial devices were still evident, with the induction of $p70^{S6k}$ phosphorylation remaining specific to stretch on the multiaxial device. These data demonstrate that the ability of C_2C_{12} myotubes to distinguish between the different types of mechanical forces that produced uniaxial and multiaxial stretch was not dependent on differences in ΔSA produced by a given amount of stretch.

Multiaxial stretch-induced phosphorylation of $p70^{S6k}$ is not localized to regions of large tensile strain. Another important difference in the mechanical forces produced by stretch on the uniaxial and multiaxial devices involved the uniformity of strains. On the uniaxial device, stretch of the culture membrane

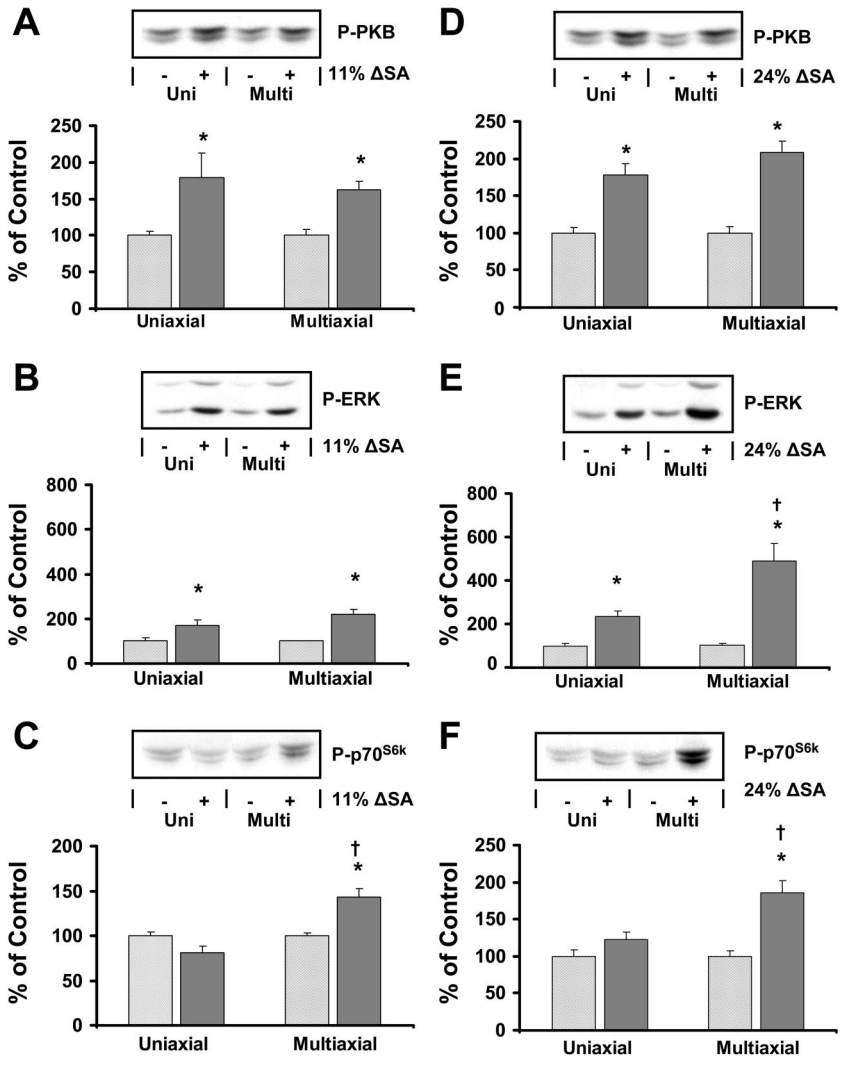

Fig. 3. Cyclic increases in culture membrane surface area, when produced by uniaxial vs. multiaxial stretch, induce different signaling events. C_2C_{12} myotubes were subjected to 10 min of 11% (*A–C*) or 24% (*D–F*) cyclic (1 Hz) membrane surface area enlargements evoked by uniaxial or multiaxial stretch. Cell homogenates were separated by SDS-PAGE, and Western blotting was performed with phosphospecific antibodies P-PKB (*A* and *D*), P-ERK (*B* and *E*), and P-$p70^{S6k}$ (*C* and *F*). Values are presented as means ± SE and expressed as a percentage of control (n = 11–13/group) from 3–4 independent experiments. Control samples are represented as light shaded bars, and stretched samples are represented as dark shaded bars. *Significantly different from control ($P \leq 0.05$). †Significantly different from uniaxial stretched samples ($P \leq 0.05$).

occurs in a uniform distribution, whereas on the multiaxial device, stretch of the culture membrane occurs in a nonuniform distribution (5, 7). The nonuniform distribution in the multiaxial device is most prominent at the outer edge of the membrane, where a rapid increase in the radial axes and a gradual decrease in the circumferential axes of tensile strain are present (Fig. 4*A*). In this region of the membrane, the magnitude of the radial tensile strain reaches more than twofold the average radial tensile strain produced across the remainder of the membrane (7). This region of large tensile strain encompasses ~10% of the membrane surface area. If the stretch-induced increase in $p70^{S6k}$ phosphorylation (85%) were localized to the area of large tensile strain, the magnitude of phosphorylation in this region would have to be 8.5-fold greater compared with the remainder of the culture membrane, a magnitude of difference that should be detectable with immunohistochemistry.

To determine whether the increase in $p70^{S6k}$ phosphorylation was localized to the region of large tensile strain, we reconstructed a composite of immunohistochemical images, extending from the periphery to the center of the well, from >50 individual images. As a positive control for the uniform distribution of staining, myotube cultures were stained with an anti-α-actinin antibody (Fig. 4, *B* and *D*). Images generated with the same phosphospecific $p70^{S6k}$ (Fig. 4, *C* and *E*) antibodies used in the Western blot analysis suggest that $p70^{S6k}$ phosphorylation was evenly distributed across the membrane as opposed to being localized to the region of large tensile strain. These data, in conjunction with the observation that $p70^{S6k}$ phosphorylation did not increase after 32% tensile strain (24% ΔSA) on the uniaxial device, support the conclusion that large magnitudes of tensile strain, resulting from the nonuniform distribution of stretch on the multiaxial device, are not responsible for the different signaling events induced by the uniaxial and multiaxial stretch devices.

Multiaxial stretch-induced phosphorylation of $p70^{S6k}$ and PKB/Akt is stimulated by distinct mechanosensory-mechanotransduction pathways. Our data indicate that multiaxial stretch-specific signaling events were induced by mechanical forces delivered through the elastic culture membrane and that these mechanical forces were not due to differences in ΔSA or localized regions of large tensile strain. To determine which mechanisms might be involved in the multiaxial stretch-specific signaling, we evaluated changes in $p70^{S6k}$ phosphorylation in myotube cultures that had been incubated with a well-known compound that disrupts the actin cytoskeleton, cytochalasin D. Disruption of the actin cytoskeleton (Fig. 5, *A* and *B*) completely blocked the multiaxial stretch-induced increase in $p70^{S6k}$ phosphorylation (Fig. 5*C*). However, disruption of the cytoskeleton had no effect on the multiaxial stretch-induced phosphorylation of PKB/Akt (Fig. 5*D*) or ERK (data not shown). These data demonstrate that signaling to $p70^{S6k}$ and PKB/Akt occurs through stimulation of distinct mechanosensory-mechanotransduction pathways and that the actin cytoskeleton is a vital component of the pathway that imparts multiaxial stretch-specific signaling to $p70^{S6k}$.

Multiaxial stretch-induced phosphorylation of $p70^{S6k}$ is not inhibited by genistein, LY-294002, PD-98059, BIM, or gadolinium. In an effort to more clearly define the signaling pathways leading to the multiaxial stretch-induced phosphorylation of $p70^{S6k}$, we incubated C_2C_{12} myotubes with pharmacological inhibitors. As noted in MATERIALS AND METHODS, the concentra-

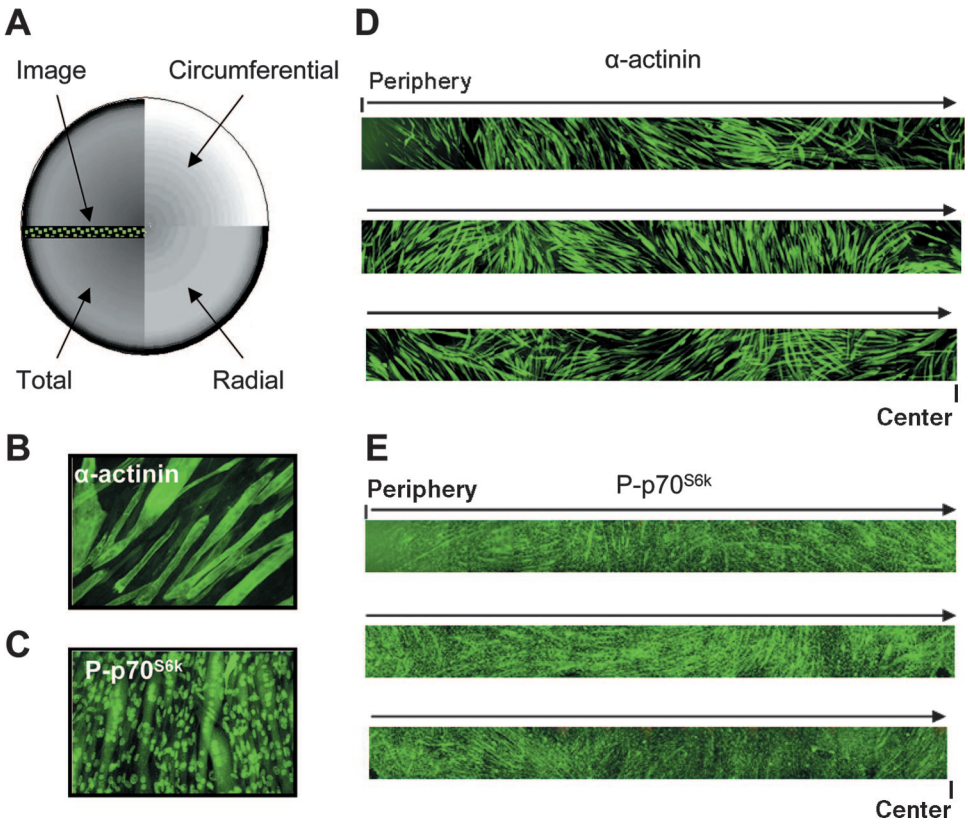

Fig. 4. Multiaxial stretch-induced phosphorylation of $p70^{S6k}$ is not localized to regions of large tensile strain. C_2C_{12} myotubes were subjected to 10 min of 15% cyclic multiaxial stretch and immediately fixed for immunohistochemistry. *A*: pictorial representation of the strains produced in the multiaxial stretch system as previously described by Gilbert et al. (7) . Increasing amounts of tensile strain are represented by an increase in the intensity of the gray scale. Circumferential tensile strain is represented in the *upper right* quadrant, radial tensile strain in the *lower right* quadrant, and total tensile strain at *left*. The rectangular inset represents the lane from which a continuous series of images extending from the periphery to the center of the well were collected. *B*: α-actinin antibody shows a high affinity for myotubes (×300 magnification). *C*: P-$p70^{S6k}$ antibody reveals a diffuse myotube and strong nuclear affinity (×300 magnification). *D*: a continuous series of images of α-actinin-stained myotubes demonstrates a uniform distribution of randomly oriented myotubes extending from the periphery to the center of the cell culture well (×60 magnification). *E*: a series of images for P-$p70^{S6k}$-stained myotubes reveals a uniform staining intensity that extends from the periphery to the center of the culture well (×60 magnification).

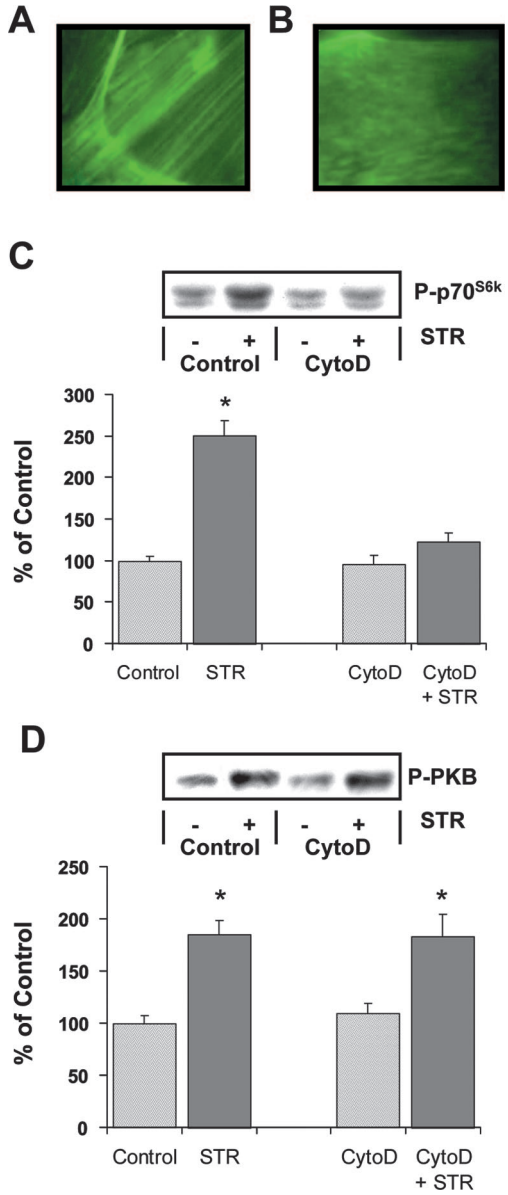

Fig. 5. Multiaxial stretch-induced phosphorylation of $p70^{S6k}$ and PKB/Akt are stimulated by distinct mechanosensory-mechanotransduction pathways. C_2C_{12} myotubes were subjected to 10 min of 15% cyclic (1 Hz) multiaxial stretch. Before (45 min) initiation of stretch (STR), culture medium was replaced with medium containing a vehicle or 10 μM cytochalasin D (CytoD). Myotubes incubated in the presence of vehicle (*A*) or CytoD (*B*) were stained with phalloidin. In the presence of vehicle, the myotubes show well-defined actin stress fibers that are abolished by CytoD (×3,000 magnification). Cell homogenates were separated by SDS-PAGE, and Western blotting was performed with P-$p70^{S6k}$ (*C*) or P-PKB (*D*) antibodies. Values are presented as means ± SE and expressed as a percentage of a static vehicle-treated sample (control) (n = 7–12/group) from 3 independent experiments. Static samples are represented as light shaded bars, and stretched samples are represented as dark shaded bars. STR, stretched samples. *Significantly different from static samples of similar treatment ($P \leq 0.05$).

tion employed for each of the inhibitors was based on several previously published reports (8, 21, 24, 29). The inhibitors tested include genistein, LY-294002, PD-98059, BIM, and gadolinium. With the exception of BIM, all of these agents altered the baseline phosphorylation of $p70^{S6k}$; however, none of these agents were able to prevent the multiaxial stretch-induced increase in $p70^{S6k}$ phosphorylation, indicating that the mechanosensory-mechanotransduction pathway leading to $p70^{S6k}$ is not fully dependent on mechanisms sensitive to these inhibitors (Fig. 6).

Multiaxial stretch-induced release of paracrine factors is not sufficient for phosphorylation of $p70^{S6k}$. To determine whether the multiaxial stretch-induced phosphorylation of $p70^{S6k}$ was due to the release of paracrine factors, we incubated static C_2C_{12} myotubes with conditioned media from stretched myotubes. The results of these experiments indicated that a stretch-induced release of paracrine factors was not sufficient for the induction of $p70^{S6k}$ phosphorylation (Fig. 7). Furthermore, the stretch-induced release of paracrine factors also was not sufficient for the induction of PKB/Akt or ERK phosphorylation (data not shown).

DISCUSSION

The initial aim of this study was to determine whether skeletal muscle cells have the fundamental ability to differentiate between different types of mechanical forces. To address this aim, we subjected skeletal myotube cultures to uniaxial or multiaxial cyclic stretch. The initial findings demonstrated that skeletal muscle cells can differentiate between uniaxial and multiaxial cyclic stretch as determined by unique increases in the phosphorylation of $p70^{S6k}$ in response to multiaxial stretch.

The mechanical forces produced during cyclic stretch include those delivered through the elastic culture membrane as well as fluid shear stress. Fluid shear results from motions in the overlying cell culture medium that, in turn, impose reactive forces (i.e., fluid shear stress) on the cells in culture. Endothelial cells are a well-known example of a cell type that is very sensitive to fluid shear forces. In particular, application of fluid shear forces on endothelial cells promotes signaling to $p70^{S6k}$ (23). In contrast, the results with C_2C_{12} myotubes demonstrated that application of fluid shear did not result in signaling changes in any of the molecules studied. This lack of a signaling response indicates that *1*) the signaling responses produced by either uniaxial or multiaxial stretch resulted primarily from changes in the mechanical forces delivered through the elastic culture membrane, and *2*) the unique signaling responses in the multiaxial vs. the uniaxial stretch system likely resulted from the different mechanical forces associated with the multiaxial stretch. In addition, the observation that C_2C_{12} myotubes did not exhibit signaling responses similar to those of endothelial cells when exposed to fluid shear stress demonstrated that mechanosensory-mechanotransduction systems exhibit cell-type specificity, and this may be associated with the unique functional demands of the cells in their tissue environment.

Further experiments were conducted to discern whether the unique response of $p70^{S6k}$ to multiaxial stretch was the result of differences in the magnitude of ΔSA (Fig. 3) or differences in localized regions of large strain (Fig. 4). These experiments demonstrated that the multiaxial stretch-specific signaling events were not a result of differences in ΔSA or localized regions of large tensile strain, and thus we propose that the multiaxial stretch-specific signaling events resulted from an intrinsic capacity of myotubes to distinguish between uniaxial and multiaxial tensile strains.

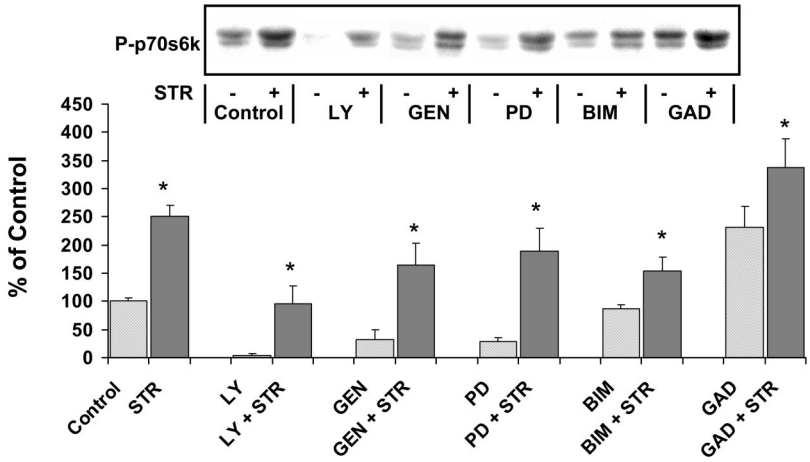

Fig. 6. Multiaxial stretch-induced phosphorylation of $p70^{S6k}$ is not dependent on tyrosine kinases, PKC, MEK, phosphatidylinositol 3-kinase (PI3K), or mechanosensitive ion channels. C_2C_{12} myotubes were subjected to 10 min of 15% cyclic (1 Hz) multiaxial stretch. Before (45 min) initiation of stretch (STR), culture medium was replaced with medium containing a vehicle (control) or 100 μM LY-294002 (LY), 250 μM genistein (GEN), 50 μM PD-98059 (PD), 20 μM bisindolylmaleimide I (BIM), or 500 μM gadolinium (III) chloride hexahydrate (GAD). Cell homogenates were separated by SDS-PAGE, and Western blotting was performed with P-$p70^{S6k}$ antibodies. Values are presented as means ± SE and expressed as a percentage of a static vehicle-treated sample (control) (n = 6–16/group). Static samples are represented as light shaded bars, and stretched samples are represented as dark shaded bars. *Significantly different from static samples of similar treatment ($P < 0.05$).

To understand how myotubes might distinguish between the different types of stretch, it is important to have a conceptual sense of the cellular architecture associated with mechanotransduction systems. Recent reports have stated that much of the cell's signal transduction machinery is physically immobilized to the cytoskeleton and is spatially integrated within the focal adhesion complex (FAC) (18, 30). Force-dependent alterations in the spatial organization of FAC signaling proteins or force-dependent changes in protein conformation could expose new binding sites and, in turn, activate signaling cascades. The cytochalasin D experiments performed in this study demonstrated that disruption of the cytoskeleton blocked the multiaxial stretch-induced signaling to $p70^{S6k}$ but had no effect on signaling to PKB/Akt, a molecule activated by both uniaxial and multiaxial stretch. These results are significant because they indicate that $p70^{S6k}$ and PKB/Akt are activated by distinct mechanosensory-mechanotransduction pathways and that the activation of these pathways is specific to the types of mechanical forces applied. In addition, they indicate that the actin cytoskeleton is a vital component of the mechanotransduction system that imparts the multiaxial stretch-specific signaling to $p70^{S6k}$. A conceptual model of an actin cytoskeleton-linked, multiaxial stretch-specific mechanosensor is described in Fig. 8.

The regulation of $p70^{S6k}$ phosphorylation is complex and involves the integration of signals from numerous pathways (31). These major pathways have been shown to include tyrosine kinases (for example, FAK), PKC, MEK, and phosphatidylinositol 3-kinase (PI3K) (6, 11, 12, 25). Thus it was surprising that the application of pharmacological inhibitors that have been reported to target these pathways did not block the multiaxial stretch-induced increase in $p70^{S6k}$ phosphorylation. Another mechanism that has been implicated in the regulation of $p70^{S6k}$ is an alteration in cellular calcium concentrations, and myotubes have been shown to contain mechanically sensitive ion channels that, when stretched, induce a calcium influx (14, 29). However, gadolinium, which has been reported to block these mechanically activated ion channels, did not inhibit the multiaxial stretch-induced increase in $p70^{S6k}$ phosphorylation, indicating that gadolinium-sensitive pathways are not required for the multiaxial stretch-induced signaling to $p70^{S6k}$. The pharmacological inhibitor studies suggest that the multiaxial stretch-induced increase in $p70^{S6k}$ phosphorylation is independent of tyrosine kinases, PKC, MEK, PI3K, and mechanically activated ion channels. These findings are consistent with the concept that multiaxial stretch induces $p70^{S6k}$ phosphorylation through a novel pathway that is distinct from the well-defined growth factor pathways (17). The results from the conditioned media experiments also indicate that the release of paracrine growth factors is not sufficient for the activation of $p70^{S6k}$ phosphorylation with multiaxial stretch. Thus the multiaxial stretch-induced signaling to $p70^{S6k}$ appears to occur through a direct mechanical mechanism. Because signaling through $p70^{S6k}$ has been implicated in the regulation of load-induced cardiac and skeletal muscle hypertrophy, a better understanding of the mechanosensory-mechanotransduction pathway leading to $p70^{S6k}$ could provide new insights into the mechanisms involved in load-induced hypertrophy (1, 33, 35)

The results of this study highlight the concept of specificity in mechanotransduction. Although this concept is only begin-

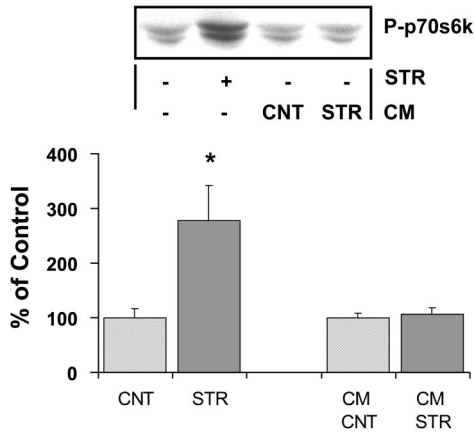

Fig. 7. Multiaxial stretch-induced release of paracrine factors is not sufficient for phosphorylation of $p70^{S6k}$. C_2C_{12} myotubes were placed in serum-free medium (serum starved) for 90 min, followed by the addition of fresh serum-free medium immediately before initiation of 10 min of 15% cyclic (1 Hz) multiaxial stretch (STR) or static conditions (CNT). The conditioned media (CM) from static or stretched myotubes was immediately removed and placed on a new set of static serum-starved myotubes for 10 min (CM CNT and CM STR, respectively). Cell homogenates were separated by SDS-PAGE, and Western blotting was performed with P-$p70^{S6k}$ antibodies. Values are presented as means ± SE and expressed as a percentage of the static samples (n = 6/group) from 2 independent experiments.

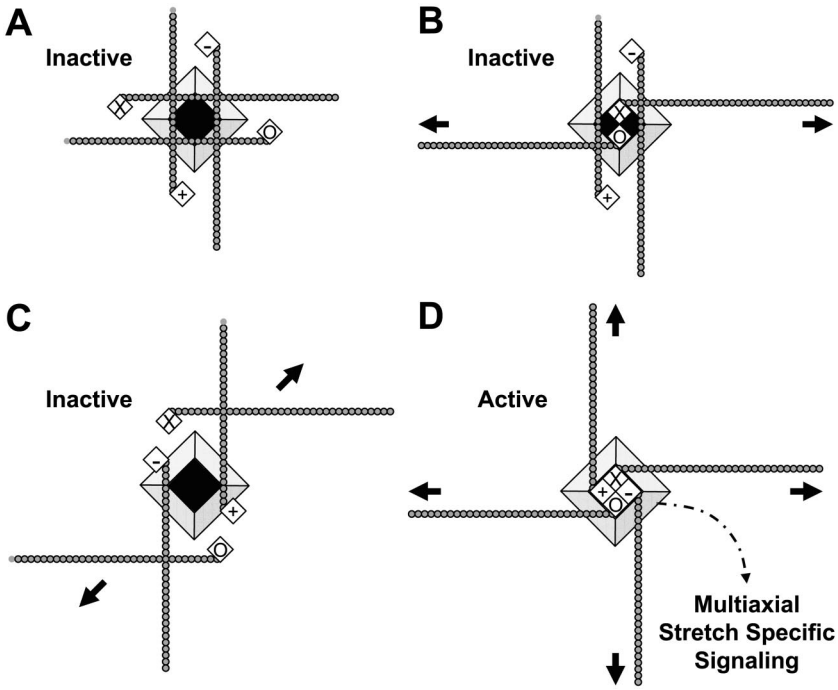

Fig. 8. Conceptual model of an actin cytoskeleton-linked, multiaxial stretch-specific mechanosensor. In this model, the actin cytoskeleton (represented as circles) is bound to focal adhesion proteins (small diamonds). In the correct configuration, the focal adhesion proteins can form a ternary diamond-shaped complex. This complex serves as a docking site that activates a multiaxial stretch-specific signaling protein (large diamond). *A*: in the resting state, the focal adhesion proteins are isolated from one another and no docking site is present. *B* and *C*: uniaxial stretch (indicated by arrows), as sensed through the actin cytoskeleton, changes the relative position of the focal adhesion proteins. The alterations in focal adhesion protein position do not produce a ternary diamond shaped complex; thus a docking site for activation of the multiaxial stretch-specific signaling protein is not formed. *D*: multiaxial stretch results in the formation of the ternary diamond-shaped focal adhesion protein complex, which allows the multiaxial stretch-specific signaling protein to dock, become activated, and, in turn, propagate multiaxial stretch-specific signaling events.

ning to be appreciated, there are some studies that have specifically addressed it. For example, differential activation of fibronectin mRNA expression and small GTPase Rac activity can be induced by tensile vs. compressive strains (20, 27); activation of G proteins is dependent on the rate of strain (13); and induction of VEGF mRNA is dependent on the magnitude of strain (34). Most similar to this study, Lee et al. (27) reported that 3% surface area deformations produced by uniaxial stretch produced an approximately 3-fold increase in fibronectin mRNA expression, whereas 3% surface deformations produced by equibiaxial stretch produced only an approximately 1.5-fold increase in fibronectin mRNA expression. The quantitatively different responses of fibronectin mRNA to uniaxial and equibiaxial stretch are very similar to the quantitatively different responses of ERK phosphorylation that we observed in response to uniaxial and multiaxial stretch. The results of this study are consistent with the examples described above and provide further evidence that cells can differentially sense specific mechanical signals that in turn elicit specific intracellular responses.

Although it is apparent that specific types of mechanical forces can induce specific cellular responses, it is not clear how this specificity arises. One possibility is that cells contain several distinct mechanosensors that are activated in response to specific mechanical stimuli. Evidence of distinct mechanosensors is lacking, but there are studies that suggest they exist. For example, MacKenna et al. (28) have shown that stretch induces JNK1 and ERK2 activation. The stretch-induced ERK2 activation is blocked with a combination of anti-α4 and -α5 antibodies and an arginine-glycine-aspartic acid (RGD) peptide, whereas stretch-induced activation of JNK1 is not blocked by these inhibitors (28). These results indicate that the mechanotransduction pathways for JNK1 and ERK2 are distinct and may involve the activation of different mechanosensors.

A recent study by Kumar et al. (24) also provides evidence that distinct mechanosensors may be contributing to results in which different types of mechanical forces activate different mechanosensory-mechanotransduction pathways. In this study, strain was applied either along the longitudinal axis of the muscle fibers or transverse to the fibers, and the result was an induction of ERK phosphorylation through different upstream pathways. This work deserves particular attention, because uniaxial stretch has been used previously to induce alignment of fusing myotubes with the longitudinal axis of the membrane (38). One consideration with the results from this study may be that uniaxial stretch, applied along the longitudinal axis, activates the common ERK cascade, as described in the study by Kumar et al. (24), whereas multiaxial stretch, being simultaneously longitudinal and transverse, represents activation of both the longitudinal and the transverse ERK cascade. In this study, the myotubes subjected to uniaxial stretch were randomly aligned, resulting in cells being subjected to a distribution of longitudinal and transverse stretch, and this feature discounts the possibility that orientation of stretch contributed to the observed differences between uniaxial and multiaxial stretch. Thus these results provide further evidence that different mechanical forces activate distinct mechanosensory-mechanotransduction pathways; whether the specificity arises through the activation of unique mechanosensors remains to be determined.

To date, the complexity of the in vivo cellular environment has limited our ability to observe specificity in mechanotransduction. However, the results of this study first clearly show that muscle cells can differentiate between uniaxial and multiaxial cyclic stretch and, second, demonstrate that specificity is a fundamental property of the mechanotransduction machinery. With the development of new analytical techniques, the ability to characterize and/or model the mechanical environment in vivo is rapidly advancing. These models are providing

new insights into how the mechanical environment is altered during the onset of pathological adaptations such as cardiac hypertrophy following a myocardial infarct and atherosclerosis (10, 26). Combining this information with the use of well-defined in vitro studies will greatly accelerate our understanding of how mechanical information is converted in specific physiological and pathological adaptations.

ACKNOWLEDGMENTS

Present addresses: T. Hornberger, Univ. of California, San Diego, Dept. of Bioengineering, La Jolla, CA 92093-0435; D. Armstrong, Dept. of Physiology, Univ. of Kentucky, Albert B. Chandler Medical Center, 800 Rose St., Lexington, KY 40536-0298.

GRANTS

This research was supported by National Institute of Arthritis and Musculoskeletal and Skin Diseases Grants AR-45617 (to K. A. Esser) and AR-48664 (to T. J. Burkholder), National Aeronautics and Space Administration Predoctoral Fellowship NGT-50406 (to T. A. Hornberger), and Pfizer funding (to K. A. Esser).

REFERENCES

1. **Bodine SC, Stitt TN, Gonzalez M, Kline WO, Stover GL, Bauerlein R, Zlotchenko E, Scrimgeour A, Lawrence JC, Glass DJ, and Yancopoulos GD.** Akt/mTOR pathway is a crucial regulator of skeletal muscle hypertrophy and can prevent muscle atrophy in vivo. *Nat Cell Biol* 3: 1014–1019, 2001.
2. **Bottlang PM, Brown TD, and Banes AJ.** Hyperelastic constitutive properties of polydimethyl siloxane cell culture membranes. In: *Advances in Bioengineering*. New York: ASME, 1993, vol. 26, p. 607–609.
3. **Brown TD, Bottlang M, Pedersen DR, and Banes AJ.** Loading paradigms—intentional and unintentional—for cell culture mechanostimulus. *Am J Med Sci* 316: 162–168, 1998.
4. **Carabello BA.** Concentric versus eccentric remodeling. *J Card Fail* 8: S258–S263, 2002.
5. **Clark CB, Burkholder TJ, and Frangos JA.** Uniaxial strain system to investigate strain rate regulation in vitro. *Rev Sci Instrum* 72: 2415–2422, 2001.
6. **Dickenson JM.** Stimulation of protein kinase B and p70 S6 kinase by the histamine H1 receptor in DDT1MF-2 smooth muscle cells. *Br J Pharmacol* 135: 1967–1976, 2002.
7. **Gilbert JA, Weinhold PS, Banes AJ, Link GW, and Jones GL.** Strain profiles for circular cell culture plates containing flexible surfaces employed to mechanically deform cells in vitro. *J Biomech* 27: 1169–1177, 1994.
8. **Goel HL and Dey CS.** Insulin stimulates spreading of skeletal muscle cells involving the activation of focal adhesion kinase, phosphatidylinositol 3-kinase and extracellular signal regulated kinases. *J Cell Physiol* 193: 187–198, 2002.
9. **Goldspink G, Scutt A, Loughna PT, Wells DJ, Jaenicke T, and Gerlach GF.** Gene expression in skeletal muscle in response to stretch and force generation. *Am J Physiol Regul Integr Comp Physiol* 262: R356–R363, 1992.
10. **Goubergrits L, Affeld K, Fernandez-Britto J, and Falcon L.** Atherosclerosis and flow in carotid arteries with authentic geometries. *Biorheology* 39: 519–524, 2002.
11. **Govindarajan G, Eble DM, Lucchesi PA, and Samarel AM.** Focal adhesion kinase is involved in angiotensin II-mediated protein synthesis in cultured vascular smooth muscle cells. *Circ Res* 87: 710–716, 2000.
12. **Graves LM, He Y, Lambert J, Hunter D, Li X, and Earp HS.** An intracellular calcium signal activates p70 but not p90 ribosomal S6 kinase in liver epithelial cells. *J Biol Chem* 272: 1920–1928, 1997.
13. **Gudi SR, Lee AA, Clark CB, and Frangos JA.** Equibiaxial strain and strain rate stimulate early activation of G proteins in cardiac fibroblasts. *Am J Physiol Cell Physiol* 274: C1424–C1428, 1998.
14. **Hannan KM, Thomas G, and Pearson RB.** Activation of S6K1 (p70 ribosomal protein S6 kinase 1) requires an initial calcium-dependent priming event involving formation of a high-molecular-mass signalling complex. *Biochem J* 370: 469–477, 2003.
15. **Henderson JH and Carter DR.** Mechanical induction in limb morphogenesis: the role of growth-generated strains and pressures. *Bone* 31: 645–653, 2002.
16. **Hornberger TA, Hunter RB, Kandarian SC, and Esser KA.** Regulation of translation factors during hindlimb unloading and denervation of skeletal muscle in rats. *Am J Physiol Cell Physiol* 281: C179–C187, 2001.
17. **Hornberger TA, Stuppard R, Conley KE, Fedele MJ, Fiorotto ML, Chin ER, and Esser KA.** Mechanical stimuli regulate rapamycin-sensitive signaling by a phosphoinositide 3-kinase-, protein kinase B- and growth factor-independent mechanism. *Biochem J* 380: 795–804, 2004.
18. **Ingber DE, Dike L, Hansen L, Karp S, Liley H, Maniotis A, McNamee H, Mooney D, Plopper G, and Sims J.** Cellular tensegrity: exploring how mechanical changes in the cytoskeleton regulate cell growth, migration, and tissue pattern during morphogenesis. *Int Rev Cytol* 150: 173–224, 1994.
19. **Jo H, Sipos K, Go YM, Law R, Rong J, and McDonald JM.** Differential effect of shear stress on extracellular signal-regulated kinase and N-terminal Jun kinase in endothelial cells. G_{i2}- and Gβ/γ-dependent signaling pathways. *J Biol Chem* 272: 1395–1401, 1997.
20. **Katsumi A, Milanini J, Kiosses WB, del Pozo MA, Kaunas R, Chien S, Hahn KM, and Schwartz MA.** Effects of cell tension on the small GTPase Rac. *J Cell Biol* 158: 153–164, 2002.
21. **Kim HP, Roe JH, Chock PB, and Yim MB.** Transcriptional activation of the human manganese superoxide dismutase gene mediated by tetradecanoylphorbol acetate. *J Biol Chem* 274: 37455–37460, 1999.
22. **Ko KS and McCulloch CA.** Intercellular mechanotransduction: cellular circuits that coordinate tissue responses to mechanical loading. *Biochem Biophys Res Commun* 285: 1077–1083, 2001.
23. **Kraiss LW, Weyrich AS, Alto NM, Dixon DA, Ennis TM, Modur V, McIntyre TM, Prescott SM, and Zimmerman GA.** Fluid flow activates a regulator of translation, p70/p85 S6 kinase, in human endothelial cells. *Am J Physiol Heart Circ Physiol* 278: H1537–H1544, 2000.
24. **Kumar A, Chaudhry I, Reid MB, and Boriek AM.** Distinct signaling pathways are activated in response to mechanical stress applied axially and transversely to skeletal muscle fibers. *J Biol Chem* 277: 46493–46503, 2002.
25. **Laser M, Kasi VS, Hamawaki M, Cooper GT, Kerr CM, and Kuppuswamy D.** Differential activation of p70 and p85 S6 kinase isoforms during cardiac hypertrophy in the adult mammal. *J Biol Chem* 273: 24610–24619, 1998.
26. **Latimer DC, Roth BJ, and Parker KK.** Analytical model for predicting mechanotransduction effects in engineered cardiac tissue. *Tissue Eng* 9: 283–289, 2003.
27. **Lee AA, Delhaas T, McCulloch AD, and Villarreal FJ.** Differential responses of adult cardiac fibroblasts to in vitro biaxial strain patterns. *J Mol Cell Cardiol* 31: 1833–1843, 1999.
28. **MacKenna DA, Dolfi F, Vuori K, and Ruoslahti E.** Extracellular signal-regulated kinase and c-Jun NH_2-terminal kinase activation by mechanical stretch is integrin-dependent and matrix-specific in rat cardiac fibroblasts. *J Clin Invest* 101: 301–310, 1998.
29. **Nakamura TY, Iwata Y, Sampaolesi M, Hanada H, Saito N, Artman M, Coetzee WA, and Shigekawa M.** Stretch-activated cation channels in skeletal muscle myotubes from sarcoglycan-deficient hamsters. *Am J Physiol Cell Physiol* 281: C690–C699, 2001.
30. **Plopper GE, McNamee HP, Dike LE, Bojanowski K, and Ingber DE.** Convergence of integrin and growth factor receptor signaling pathways within the focal adhesion complex. *Mol Biol Cell* 6: 1349–1365, 1995.
31. **Pullen N and Thomas G.** The modular phosphorylation and activation of p70s6k. *FEBS Lett* 410: 78–82, 1997.
32. **Russell B, Motlagh D, and Ashley WW.** Form follows function: how muscle shape is regulated by work. *J Appl Physiol* 88: 1127–1132, 2000.
33. **Shioi T, McMullen JR, Tarnavski O, Converso K, Sherwood MC, Manning WJ, and Izumo S.** Rapamycin attenuates load-induced cardiac hypertrophy in mice. *Circulation* 107: 1664–1670, 2003.
34. **Suzuma I, Suzuma K, Ueki K, Hata Y, Feener EP, King GL, and Aiello LP.** Stretch-induced retinal vascular endothelial growth factor expression is mediated by phosphatidylinositol 3-kinase and protein kinase C (PKC)-ζ but not by stretch-induced ERK1/2, Akt, Ras, or classical/novel PKC pathways. *J Biol Chem* 277: 1047–1057, 2002.
35. **Thomas G and Hall MN.** TOR signalling and control of cell growth. *Curr Opin Cell Biol* 9: 782–787, 1997.
36. **Ueyama T, Kawashima S, Sakoda T, Rikitake Y, Ishida T, Kawai M, Yamashita T, Ishido S, Hotta H, and Yokoyama M.** Requirement of activation of the extracellular signal-regulated kinase cascade in myocardial cell hypertrophy. *J Mol Cell Cardiol* 32: 947–960, 2000.
37. **Vandenburgh H and Kaufman S.** In vitro model for stretch-induced hypertrophy of skeletal muscle. *Science* 203: 265–268, 1979.
38. **Vandenburgh HH and Karlisch P.** Longitudinal growth of skeletal myotubes in vitro in a new horizontal mechanical cell stimulator. *In Vitro Cell Dev Biol* 25: 607–616, 1989.